

Monitoring of DNA structural changes after incorporation of the phenylpyrazole insecticide fipronil

Valéria Verebová^a, Zdenka Bedlovičová^a, Zuzana Bednáríková^b, Jana Staničová^{a,c,*}

^a Department of Chemistry, Biochemistry and Biophysics, University of Veterinary Medicine & Pharmacy, Komenského 73, 040 01, Košice, Slovakia

^b Department of Biophysics, Institute of Experimental Physics, Slovak Academy of Science, Watsonova 1935/47, 040 01, Košice, Slovakia

^c Institute of Biophysics and Informatics, First Faculty of Medicine, Charles University, Kateřinská 1, Prague, Czech Republic

ARTICLE INFO

Keywords:

Insecticides
Fipronil
DNA structure and stability
Incorporation

ABSTRACT

The use of insecticides presents a risk to the environment because they can accumulate in the water, soil, air, and organisms, endangering human and animal health. It is therefore essential to investigate the effects of different groups of insecticides on individual biomacromolecules such as DNA. We studied fipronil, which belongs to the group of phenylpyrazole insecticides. The interaction of fipronil with calf thymus DNA was investigated using spectroscopic methods (absorption and fluorescence spectroscopy) complemented with infrared spectroscopy and viscosity measurement. Fluorescence emission spectroscopy showed the formation of a fipronil/DNA complex with a combined static and dynamic type of quenching. The binding constant was 4.15×10^3 L/mol. Viscosity changes were recorded to confirm/disconfirm the intercalation mode of interaction. A slight change in DNA viscosity in the presence of fipronil was observed. The phenylpyrazole insecticide does not cause significant conformational changes in DNA structure or increase of its chain length. We hypothesize that fipronil is incorporated into the minor groove of the DNA macromolecule via hydrogen interactions as indicated by FT-IR and CD measurements.

1. Introduction

Due to increasing resistance to insecticides and their adverse effects on public health, older groups (e.g., carbamates, organophosphates, organochlorine compounds, and pyrethroids) are gradually being replaced by new families of insecticides. Among these, neonicotinoids and phenylpyrazoles are the most used [1]. Fipronil (FIP) is a relatively new phenylpyrazole insecticide introduced for pest control. It is an extremely neurotoxic insecticide with good selectivity among insects and mammals. FIP was discovered and developed in the 1980s and marketed in 1993. This compound is contained in formulations such as Regent® and Frontline®. FIP is an insecticide with good stomach toxicity and is used to control many soil and foliar insects (e.g., potato caterpillars) that are parasitic on various crops, particularly maize and turf, and for public health insect control. It is also used for seed treatment and as a bait for cockroaches, ants, and termites. A considerable advantage is that FIP is effective against pyrethroid-resistant or tolerant insects, organophosphate and carbamate insecticides [2].

The chemical name of FIP (Fig. 1) is 5-amino-1-[2,6-dichloro-4-(trifluoromethyl)phenyl]-4-[(trifluoromethyl)sulphonyl]-1*H*-pyrazole-3-

carbonitrile. This compound contains a trifluoromethyl sulphonyl group at the 4th position, which gives this molecule a higher liposolubility, facilitating its deposition in adipose tissue and contributes to its prolonged action in the body. The solubility of FIP in water is 2.4 mg/L at pH 5 and 22 mg/L at pH 9. Its density is higher than the density of water. FIP does not leak because of its relatively low vapor pressure and is found in the air only when used in spray form. The insecticide we studied is characterized by low mobility in soil, resulting in a low contamination potential and a tendency to disperse, thereby facilitating its degradation by microorganisms [3].

Considering the 3-cyano and 4-trifluoromethyl sulphonyl group of phenylpyrazole as key pharmacophores, several FIP derivatives have been developed by modifying the amino group to pyrazole [4]. Mechanism of FIP action is based on blocking γ -aminobutyric acid chloride and glutamate chloride channels which leads to disruption of the central nervous system of insects [5], hyperexcitation, and death [6]. The target-site specificity of FIP on insect channels is probably the reason for its higher toxicity to insects compared to mammals [7,8]. FIP's sulfonic metabolites and photodegradation products (fipronil desulfinyl) pose a higher risk to insects, mammals, fish, birds, and being more toxic to

* Corresponding author. Institute of Biophysics and Informatics, First Faculty of Medicine, Charles University, Kateřinská 1, Prague, Czech Republic
E-mail address: jana.stanicova@lfi.cuni.cz (J. Staničová).

them than FIP itself [6]. FIP has been found to be toxic to a large number of birds and to most fish species. It has been shown to exert sub-lethal, cytotoxic, and genotoxic effects and to impair immune function, to reduce growth and reproductive success, often at concentrations below those associated with mortality. Indirect effects are rarely taken into account in the risk assessment process. Reductions in invertebrate abundance caused by FIP use have been shown to affect the growth of one fish species. In other cases, reductions in lizard populations have been linked to FIP effects on termite prey. It is therefore confirmed that FIP can have direct and indirect effects on terrestrial and aquatic wild vertebrates, and further investigation of its environmental safety is, therefore, necessary [5]. Chronic exposure of rats to FIP has demonstrated its toxic effects on the thyroid, liver, and kidneys [9]. Cyclic, systemic applications of fipronil have bio accumulative effects which in turn affect all animals along the trophic chain [10]. The World Health Organization has classified fipronil as a moderately toxic insecticide as an increased incidence of seizures and altered thyroid hormone levels have been reported, especially in rats (Badgular et al., 2017).

FIP has been found to cause a variety of sub-organ damage (kidney, brain, and liver of mice [11], represented by levels of markers of oxidative stress such as SOD (superoxide dismutase), GST (glutathione-S-transferase), CAT (catalase), and TBARS (thiobarbituric acid reactive substances). SOD and CAT represent the major components of the antioxidant enzyme system in insects. Antioxidant enzyme systems protect cells from oxidative disorders, protein and DNA damage, and lipid peroxidation. *In vitro* and *in vivo* (e.g. birds) studies indicated that DNA damage has been observed after exposure to FIP [12,13]. The damage of DNA *in vitro* was demonstrated by the comet assay [14]. The oxidative damage induced in DNA by FIP is little known [15]. FIP exhibits mutagenic effects in rats [16]. Vitamin E is considered to be the most promising vitamin in reducing genotoxic effects induced by chemicals as well as pesticides [17]. Exposure to fipronil in mice caused a significant increase in the frequency of micronuclei in polychromatic erythrocytes. Similarly, structural chromosomal aberrations in bone marrow cells and DNA damage in lymphocytes were found to be significantly higher in fipronil-exposed rats compared with their respective controls. The degree of protection from fipronil-induced genotoxicity was demonstrated by vitamin E pretreatment, as follows 63.28 % for chromosomal aberrations; 47.91 % micronucleus formation; and 74.70 % for DNA damage. The results of this study demonstrate the genotoxic nature of fipronil and document the protective role of vitamin E [18].

Uncontrolled use of insecticides such as FIP and neonicotinoids can affect population dynamics at both structural and functional levels. Appropriate scientific use of insecticides together with a well-studied mechanism of action can significantly reduce adverse effects in the population [19]. Fipronil is similar in popularity to systemic insecticides - neonicotinoids because it is applied to plants by a wide range of methods, from sprays to seed treatments and soil drenches. Like neonicotinoids, it is characterized by high toxicity to invertebrates. It also increases the likelihood of environmental contamination and exposure of non-target organisms as neonicotinoids. Environmental contamination can occur in several ways, including dust arising from the sowing of

treated seeds, contamination and accumulation in arable soils and soil water, runoff into waterways, and uptake of pesticides by nontarget plants via their roots or dust deposition on leaves [20].

Our study is expected to provide an important insight into DNA interactions with FIP. We studied this binding using spectroscopic methods including absorbance, fluorescence, and circular dichroism complemented with FTIR and viscosity measurements. This investigation might be beneficial in cases of frequent application of FIP as an insecticide. In addition, our results may provide data necessary for clarification of the binding mechanisms of FIP with DNA and may be also be useful for environmental and food safety, as well as human and animal health protection when FIP is used as an insecticide.

2. Materials and methods

2.1. Chemicals and reagents

FIP (CAS Number 120068-37-3) with 99 % purity and calf thymus DNA were purchased from Sigma Aldrich (Darmstadt, Germany). A stock solution of FIP (10^{-2} mol/L) was prepared by dissolving in ethanol. DNA was dissolved in Tris-EDTA buffer (TE, 10 mmol/L Tris, 1 mmol/L EDTA) and its pH was adjusted to 7.4 by slowly adding 1 mol/L hydrochloric acid. The TE buffer solution was filtered on MillexGV (0.22 μ m) filter before measurement. Ethidium bromide solution (EtBr, CAS Number 1239-45-8) with 95 % purity was purchased from Sigma-Aldrich (Darmstadt, Germany) with a 1.3×10^{-2} mol/L concentration. FIP stock solution, DNA, and TE buffer solution were stored at 4 °C.

2.2. UV-Vis studies

Absorption measurements were performed on a Cary 60 UV-Vis spectrophotometer (Agilent Technologies, USA) using a quartz cuvette with a 1-cm path length at laboratory temperature. The concentration of the DNA stock solution was calculated by measuring the absorbance at 260 nm as 2.4×10^{-3} mol/L. The absorption titration experiment was carried out at a constant FIP concentration of 2×10^{-5} mol/L, and the DNA concentration was varied during the measurement in the interval from 1×10^{-5} mol/L to 4×10^{-5} mol/L. All samples were stabilized before measurement for 10 min. The measurements were performed in the range of 200–800 nm.

2.3. Fluorescence measurements

The fluorescence binding experiment was carried out with a spectrofluorimeter RF-5301 PC (Shimadzu, Japan). The width of the excitation and emission slit was 5nm/5 nm. Fluorescence spectra of FIP (3×10^{-5} mol/L) and FIP/DNA complexes with different DNA concentrations (2.4×10^{-5} – 3×10^{-4} mol/L) were obtained by recording fluorescence in the spectral region of 300–700 nm after excitation at 280 nm. The interaction of FIP with DNA was studied in the spectral range 370–550 nm and its analysis was performed at 450 nm. All complexes were stabilized before the experiment for 10 min at laboratory temperature.

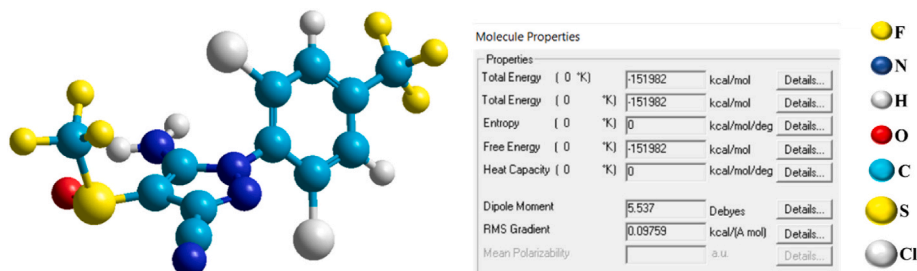


Fig. 1. Chemical structure of FIP and the magnitude of its dipole moment.

2.4. DNA melting studies

DNA denaturation was performed using an absorption spectrophotometer Cary 60 UV-Vis (Agilent Technologies, USA) with an attached Peltier module, which is used for continuous temperature change. DNA melting temperatures of 3×10^{-5} mol/L and DNA/FIP complexes at 1/1 and 1/2 ratios were determined by monitoring the absorption intensity of the 260 nm absorption band at different temperatures. During the measurement, the temperature was continuously increased in the range of 20–95 °C in 5 °C increments. The concentration of FIP was varied during the measurement from 3×10^{-5} mol/L to 6×10^{-5} mol/L. We sealed the top of the cuvette with parafilm to prevent excessive evaporation of the samples. All samples were stabilized for 10 min.

2.5. Viscosity test

The viscosity of the DNA solution was measured at 298.1 ± 0.2 K using an Ostwald viscometer and thermostatic water bath. DNA/EtBr and DNA/FIP solutions were prepared in TE buffer (pH = 7.4). For viscosity measurements, we used DNA in a concentration of 5×10^{-5} mol/L and the DNA/EtBr and DNA/FIP complexes in ratios of 1/0; 1/0.5; 1/1; 1/1.5, and 1/2. EtBr and FIP concentrations were varied in the interval 2×10^{-5} – 1×10^{-4} mol/L. The flow time of DNA and the different DNA/EtBr and DNA/FIP complexes through the capillaries of the viscometer was recorded by digital timers with an accuracy of ± 0.02 s. DNA and all DNA/EtBr and DNA/FIP complexes were measured 15 times, and the mean value was calculated. In this experiment, the samples were equally stabilized for 10 min prior to the measurements.

2.6. FT-IR spectra analysis

FT-IR spectra of FIP, and DNA samples free at a concentration of 10^{-2} mol/L and 1.5×10^{-2} mol/L, respectively, or in the FIP/DNA complex with a concentration ratio of 1/5, ($c(\text{FIP}) = 2.4 \times 10^{-3}$ mol/L; $c(\text{DNA}) = 12 \times 10^{-3}$ mol/L) were recorded using a Nicolet™ 8700 Fourier transform infrared spectrometer (Thermo Scientific) equipped with a Smart OMNI-Sampler (diamond crystal). 5 μL of a sample was spread on the diamond surface. Two measurements were taken for each sample. Each spectrum represents an average of 128 repetitions, recorded in the region between 1800 and 700 cm^{-1} with a resolution of 2 cm^{-1} . The recorded spectra were smoothed by means of OMNIC8 software (Thermo Fisher Scientific). The spectra were subsequently deconvoluted using the peak analyzer in OriginPro 8.5 (OriginLab Corporation). The baseline was subtracted and the peak positions were manually added in correlation with the raw data. The difference spectra [(DNA solution + FIP) – FIP] were obtained using the sharp band at 970 cm^{-1} as an internal reference.

2.7. Circular dichroism measurements

CD measurements of DNA in the presence of FIP after 10 min stabilization were recorded using a Jasco J-810 CD spectropolarimeter (Jasco, Easton, MD, USA). The CD experiments were performed in Tris-HCl buffer (0.1 mol/l Tris, 0.1 mol/l HCl; pH 7.4) at laboratory temperature. The CD spectra represent the automatic average of three consecutive scans. Measurements in the UV region (230–320 nm) were performed with a 1 mm path length rectangular quartz cell at a scan rate of 100 nm/min. The optical chamber of the CD spectrometer was deoxygenated with dry nitrogen before use and kept in a nitrogen atmosphere during the experiments. CD spectra were recorded for different complexes of DNA/FIP in ratio 1/0, 1/1, 1/2, and 1/3. All observed CD spectra were corrected for the buffer signal and presented without smoothing or further data processing.

All spectra and graphs from individual experiments were processed and analyzed using Origin 6.0 and 9.0. DNA denaturation curves were created and evaluated in Graphit.

3. Results and discussion

3.1. UV-Vis studies

Absorption spectroscopy is a fundamental method for better investigating the physicochemical properties of FIP and its interaction with DNA macromolecules. The purity of DNA was monitored by measuring the absorbance ratio at 260 and 280 nm. DNA solution has an A_{260}/A_{280} ratio >1.8 , indicating that the DNA was free of the presence of protein [21]. FIP is characterized by two absorption maxima in the ultraviolet region of the electromagnetic spectrum at wavelengths of 204 and 280 nm.

FIP is known to dissolve well in organic solvents. In aqueous media, it dissolves sufficiently, but its solubility is lower than in an organic solvent. Using the HyperChem 8.0 program (Hypercube, Inc. [22]), we created a structural model of FIP (Fig. 1) and calculated its dipole moment by the semi-empirical AM1 method [23]. The dipole moment is a vector physical quantity describing the asymmetric distribution of electric charge in a molecule and is used to determine the polarity of a given molecule. The magnitude of the FIP dipole moment is 5.537 D, i.e. 1.85×10^{-29} C m, proving the polar behavior of FIP, which dissolves well in polar solvents, which is consistent with what is known about solubility. The structural model clearly shows that the FIP molecule is not planar. It has a crescent shape, caused by the sulphur atom being drawn inside the molecule. The sulphur atom, due to its position, does not significantly affect the polarity of the FIP. The polarity of FIP is mainly influenced by the six fluorine atoms located at opposite ends of the molecule, which contribute to the formation of the crescent structure of FIP. The high polarity of FIP is presumably suitable for the formation of hydrogen bonds in the groove of the DNA molecule.

The binding of FIP to the DNA macromolecule was characterized by absorption titration. Fig. 2a shows the absorption spectrum of FIP with a concentration of 2×10^{-5} mol/L in TE buffer and FIP/DNA complexes in different ratios (1/0.5; 1/0.6; 1/0.8; 1/1; 1/1.5; 1/2), while the DNA concentration was varied from 10^{-5} mol/L to 4×10^{-5} mol/L. By increasing the DNA concentration, we observed an increase in the intensity of the FIP absorption band at 280 nm.

It is well known that small ligands, such as pharmaceuticals and pesticides, can be incorporated into DNA non-specifically in two ways, either by intercalation or by binding to the groove [24]. Intercalation with DNA is interacted by planar aromatic positively charged molecules that incorporate between the nitrogenous bases of DNA. The groove binding is characterized by ligand anchoring close to the sugar-phosphate chain [25]. Binding of the ligand to DNA via intercalation is indicated by a change in absorbance (hypochromism – decrease of absorbance) due to an intercalation mode involving a “stacking” interaction between the aromatic chromophore and DNA base pairs [26]. This is a strong interaction of the electron shell of the intercalating molecule with the electron shell of the nitrogenous DNA bases [27]. By observing changes in the absorption spectrum of FIP as the concentration of DNA gradually increased, we did not observe a hypochromic effect on the FIP absorbance intensity. On the contrary, we detected an increase in absorbance intensity, i.e. a hyperchromic effect. This allows us to predict that FIP does not interact with DNA by means of intercalation, but rather in some other way. It is likely that this interaction takes place through hydrogen bridges or electrostatic forces [28].

The binding strength of FIP and DNA is expressed by the internal binding constant (K_b), which was determined by monitoring changes in FIP absorbance with increasing DNA concentration according to the following equation (1)

$$\frac{[DNA]}{\varepsilon_a - \varepsilon_f} = \frac{[DNA]}{\varepsilon_b - \varepsilon_f} + \frac{1}{K_b(\varepsilon_b - \varepsilon_f)} \quad (1)$$

where [DNA] is the DNA concentration converted to bp number. Apparent absorbance coefficients ε_a , ε_f , and ε_b are attributed to the

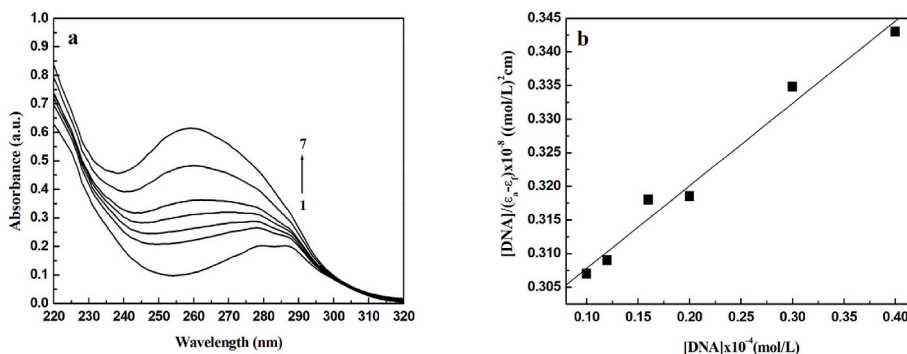


Fig. 2. a Absorption spectra of FIP (2×10^{-5} mol/L) after addition of DNA (10^{-5} – 4×10^{-5} mol/L) in TE buffer pH 7.4, lines 1–7: c (FIP/DNA) = 1/0, 1/0.5, 1/0.6, 1/0.8, 1/1, 1/1.5, 1/2 respectively. The arrow indicates the change in absorbance with increasing DNA concentration. **b** The linear dependence of $[\text{DNA}]/(\epsilon_a - \epsilon_f)$ vs. $[\text{DNA}]$ was used to calculate the binding constant.

$A_{\text{measured}}/[\text{FIP}]$ ratio, the extinction coefficient for free FIP, and FIP completely bound to DNA. We constructed a plot of the $[\text{DNA}]/(\epsilon_a - \epsilon_f)$ vs. $[\text{DNA}]$ linear dependence (Fig. 2b) with a straight-line directive of $1/(\epsilon_b - \epsilon_f)$ and an offset (intercept on the y-axis) $1/[K_b(\epsilon_b - \epsilon_f)]$. We calculated the value of the binding constant K_b from the ratio of the directive and displacement of the constructed linear dependence [19]. The magnitude of the binding constant is 4.15×10^3 L/mol.

When comparing the calculated FIP binding constant with those of typical intercalating agents such as EtBr ($K_b = 1.4 \times 10^6$ L/mol) [29], quinizarin ($K_b = 3.2 \times 10^7$ L/mol) and danthrone ($K_b = 7.2 \times 10^6$ L/mol) [30], the values of the intercalators binding constants are orders of magnitude higher. Based on these results, the FIP does not intercalate to the DNA macromolecule. We can also rule out binding via weak electrostatic forces since the values of the binding constants attributed to this type of interaction are low (on the order of 10^2) [31,32]. We hypothesize that FIP does not bind to the surface of the DNA macromolecule by electrostatic forces or intercalation. A more likely mode of FIP incorporation into DNA is its binding to the DNA groove.

3.2. Fluorescence measurements

To complement the specific nature of FIP binding to DNA, we performed fluorescence measurements by monitoring the emission curves of FIP in the absence and presence of DNA (Fig. 3a). Upon excitation at 280 nm, the FIP fluorescence spectrum shows a pronounced emission maximum at a wavelength of 450 nm. The concentration of FIP was constant (3×10^{-5} mol/L), and the concentration of DNA varied in the interval from 2.4×10^{-5} to 3×10^{-4} mol/L. In the presence of DNA, we observe a decrease in the intensity of FIP fluorescence. These results suggest that the FIP fluorescence is quenched by DNA as binding between FIP and DNA occurs [33,34]. An increase in FIP emission by DNA

would indicate the aggregation or intercalation of FIP into DNA [35]. Considering the observed decrease in fluorescence intensity, we can exclude the formation of FIP aggregates and assume that FIP interacts with DNA in a binding mode other than intercalation.

Moreover, in the presence of DNA, a leftward shift of the FIP fluorescence intensity maximum is observed (approximately 10 nm), i.e. a shift to lower wavelengths of the electromagnetic spectrum. This hypsochromic effect may be caused by environmental factors immediately surrounding the FIP, such as differences in polarity, hydrophobicity, hydrophilicity, pH, or the presence of electrostatic charges [36,37]. A change in polarity is likely to occur when the FIP is less exposed to the solvent.

To confirm the formation of the FIP/DNA complex, we examined the fluorescence quenching in more detail. In general, fluorescence quenching involves several mechanisms, such as dynamic quenching, static quenching, and combined dynamic and static quenching. Contact between the fluorophore (energy-absorbing substance) and the quencher is the prerequisite for dynamic and static quenching. In dynamic quenching, the quencher (in our case, DNA) should be in contact with the fluorophore (FIP) for a period equal to the lifetime of the excited state, and after contact, the fluorophore returns to the ground state without radiating energy (without emission). In dynamic quenching, there is no permanent change in the structure of the molecule. Static quenching is characterized by the forming of a non-fluorescent complex between the fluorophore and the quencher [38]. Whether the quenching mechanism corresponds to combined dynamic and static quenching can be characterized by the Stern-Volmer equation (2)

$$\frac{F_0}{F} = (1 + K_{SV}[Q])(1 + K_b[Q]) \quad (2)$$

where K_b is the binding (or static quenching) constant, while the

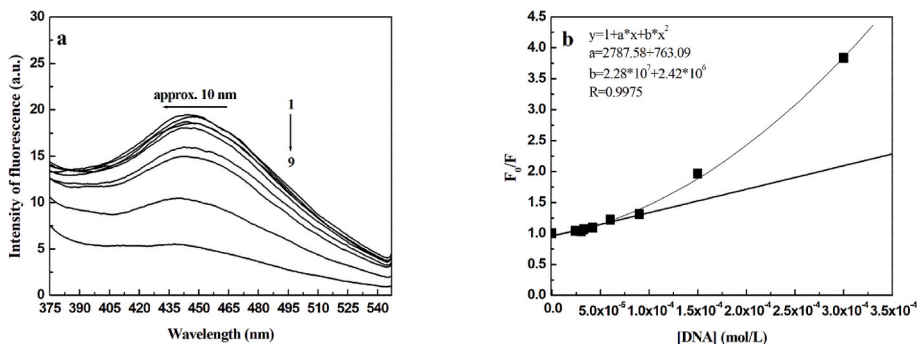


Fig. 3. a The fluorescence spectra of FIP (3×10^{-5} mol/L) after the addition of DNA (2.4×10^{-5} – 3×10^{-4} mol/L) in TE buffer pH 7.4, lines 1–9: c (FIP/DNA) = 1/0, 1/0.8, 1/1, 1/1.1, 1/1.4, 1/2, 1/3, 1/5 and 1/10 respectively. The arrow indicates the fluorescence changes with increasing DNA concentration. **b** Stern-Volmer dependences of FIP/DNA complexes at laboratory temperature.

quenching constant K_{SV} corresponds to the dynamic quenching. This modified form of the Stern-Volmer equation is the second-order equation for the $[Q]$ quencher concentration. Fig. 3b represents the Stern-Volmer dependence of F_0/F vs. $[Q]$ (F_0 – fluorescence intensity of FIP in the absence of DNA; F – fluorescence intensity of FIP in the presence of DNA) of the FIP/DNA system at laboratory temperature [39]. We detected a non-linear dependence of F_0/F vs. $[Q]$ pointing to a combined dynamic and static quenching of FIP molecules in the presence of DNA.

Fig. 3b shows that the Stern-Volmer dependence is linear for concentrations of DNA $< 9 \times 10^{-5}$ mol/L and demonstrates a positive deviation from linearity at higher DNA concentrations, too. These observations are consistent with the available literature [39] and suggest that dynamic quenching occurs only at low quencher (DNA) concentrations. Second-order polynomial regression of the obtained experimental results showed a very high correlation coefficient R ($R = 0.997$). The solution of the second-order equation did not lead to obtaining specific constants K_b and K_{SV} , so we determined the Stern-Volmer quenching constant (K_{SV}) only from the linear part of the dependence. The value of K_{SV} had a value of 3796 L/mol.

The results obtained by fluorescence measurements allow us to assume that FIP interacts with DNA in a non-intercalating manner. The interaction of FIP with DNA may be a result of contact of FIP with DNA during the lifetime of the excited state of FIP, without any changes in the structure of the interacting molecules. In higher DNA concentrations, we observed static quenching of FIP fluorescence in the presence of DNA, forming a non-fluorescent complex.

3.3. DNA melting studies

When a DNA molecule is exposed to extreme pH or heat, the molecule of DNA undergoes conformational changes from an ordered double helix structure into a random single-stranded form at melting temperature (T_m). The melting temperature can change by the interaction of DNA with small molecules [40]. Therefore, we studied DNA (c (DNA) = 3×10^{-5} mol/L) denaturation in the absence of FIP and for DNA/FIP complexes (DNA/FIP = 1/1, 1/2) with increasing FIP concentration (c (FIP) = 3×10^{-5} – 6×10^{-5} mol/L). DNA denaturation is also associated with changes in the thermodynamic parameters T_m , ΔT , and ΔH .

The measured curves were used to calculate the basic thermodynamic parameters. By monitoring the changes in DNA absorbance intensity at 260 nm as a function of increasing temperature, the

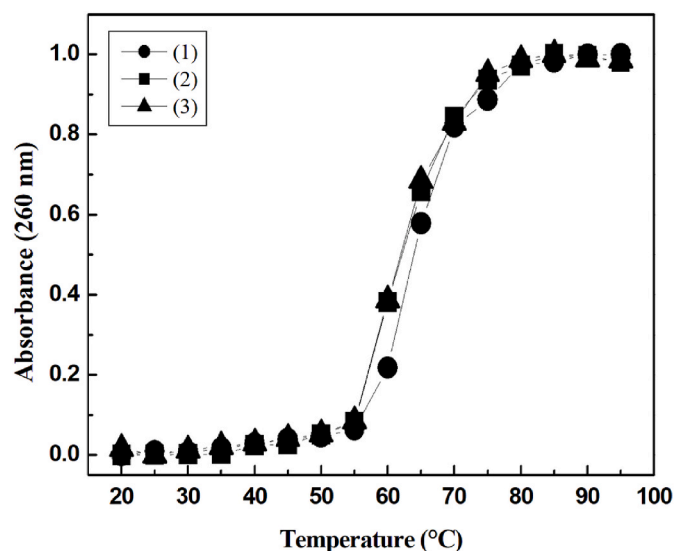


Fig. 4. Normalized melting curves of free DNA (1) and in complex with FIP in concentration ratios 1/1 (2) and 1/2 (3), c (DNA) = 3×10^{-5} mol/L and c (FIP) = 3×10^{-5} – 6×10^{-5} mol/L.

normalized melting curves (Fig. 4) were constructed and fitted using the Van't Hoff equation [41].

$$A = A_{min} + \frac{A_{max} - A_{min}}{1 + e^{\left[\frac{\Delta H}{R} \times \left(\frac{1}{T} - \frac{1}{T_m} \right) \right]}} \quad (3)$$

where A is the absorbance, A_{min} and A_{max} represent the minimum and maximum measured absorbance, T_m is the melting temperature and T is the actual temperature, H is the enthalpy of the helix-coil transition, and R is the gas constant. The helix-coil transition is also characterized by the width of the temperature interval ΔT obtained by constructing a tangent to the melting curve. Using the tangent line, we have determined temperatures T_1 , T_2 , and ΔT . T_1 represents the initial temperature of the helix-coil transition when 17 % of the base pairs of the DNA molecule are unraveled. The temperature T_2 is the final transition temperature corresponding to 83 % of disordered base pairs. The thermodynamic quantity, the width of the temperature interval ΔT , is calculated from the relation [42].

$$\Delta T = T_2 - T_1 \quad (4)$$

All calculated thermodynamic parameters are summarized in Table 1.

Intercalation of ligands into the DNA structure leads to stabilization of nitrogenous bases, which is characterized by an increase of the melting temperature T_m by approximately 5–8 °C in the presence of small molecules during DNA denaturation. Conversely, a binding mode other than intercalation (such as electrostatic interaction on the DNA surface (we ruled out this type of binding based on the results of the absorption titration experiment) or binding into the groove) does not cause an increase in melting temperature [43]. Our measured results indicate that in the presence of FIP in the DNA solution, there is a decrease in melting temperature of almost 2 °C (from 64.22 °C corresponding to pure DNA to 62.24 °C for the DNA/FIP complex = 1/2). Similarly, we observed a decrease in the Van't Hoff enthalpy with increasing FIP concentration. The width of the temperature interval had the same trend, i.e., we obtained a decrease in its value (from 21.81 °C for DNA to 20.78 °C for the DNA/FIP complex = 1/2) in the presence of FIP. We detected a decrease in the individual DNA values of thermodynamic parameters after adding FIP to the DNA solution, suggesting DNA denaturation. The observed decrease in melting temperature is less than 5 °C, indicating that FIP interacts with DNA in a mode other than by intercalation. We hypothesize that the binding of FIP to DNA may occur via electrostatic forces on the surface of the molecule or by incorporation of FIP into the groove of the DNA macromolecule. Observed changes in thermodynamic parameters lead us to conclude that FIP destabilizes DNA due to its interaction with the groove [44].

It is known from the literature that ligands containing at least two aromatic rings that are joined by a flexible bond (allowing torsion) will bind to the minor groove of DNA preferentially to regions rich in A-T pairs [45,46]. This has been shown for interactions of neonicotinoid-type pesticide (e.g., thiacloprid) with DNA, as evidenced by the biphasic shape of the DNA melting curves [47]. Since we did not observe the biphasic nature of the melting curves, we cannot specify whether FIP is incorporated into the minor or major DNA groove.

Table 1

Thermodynamic parameters determined from the melting curves of free DNA and DNA/FIP complexes.

	T_m (°C)	T_1 (°C)	T_2 (°C)	ΔT (°C)	ΔH (kJ/mol)
DNA	64.24	53.26	75.07	21.81	265.51 ± 0.17
DNA/FIP = 1/1	62.33	50.70	72.03	21.33	246.92 ± 0.16
DNA/FIP = 1/2	62.24	51.24	72.02	20.78	239.74 ± 0.14

Table 2

Main experimental wavenumbers of DNA, FIP, complex FIP/DNA, difference [(DNA solution + FIP) – FIP] vibrations as obtained by FT-IR spectroscopy and their assignments.

DNA		Difference spectrum FIP/DNA $r = 1/5$		FIP		FIP/DNA 1/5
Wavenumber (cm ⁻¹)	Assignment	Wavenumber (cm ⁻¹)	Wavenumber (cm ⁻¹)	Assignment	Wavenumber (cm ⁻¹)	Wavenumber (cm ⁻¹)
840 <i>m</i>	phosphodiester mode		883 <i>s</i>	heterocycle ν		877 <i>s</i>
894 <i>m</i>	sugar-phosphate stretch	899 <i>m</i>	1049 <i>vs</i>	S=O ν		1045 <i>vs</i>
970 <i>s</i>	C–C deoxyribose stretch	970 <i>s</i>	1090 <i>s</i>	heterocycle ν		1085 <i>s</i>
1054 <i>s</i>	C–O deoxyribose stretch	1042 <i>s</i>	1143 <i>m</i>	C–F ν		
1086 <i>vs</i>	symmetric PO ₂ ⁻ stretch	1084 <i>vs</i>	1188 <i>m</i>	C–F ν		
1222 <i>s</i>	asymmetric PO ₂ ⁻ stretch	1221 <i>s</i>	1323 <i>m</i>	aromatic cycle-NH ₂ ν		1321 <i>m</i>
1489 <i>m</i>	in-plane vibration of cytosine	1481 <i>m</i>	1376 <i>m</i>	C=C in heterocycle ν		1383 <i>m</i>
1617 <i>m</i>	adenine (C7=N stretching)	1628 <i>m</i>	1467 <i>m</i>	-C=C–N ν		1467 <i>m</i>
1652 <i>s</i>	thymine (C2=O stretching)	1662 <i>s</i>	1582 <i>w</i>	C=C in ring ν		1582 <i>w</i>
1714 <i>s</i>	guanine (C=O stretching)	1708 <i>s</i>				

Note: Relative intensities: *vs* – very strong, *s* – strong, *m* – medium, *w* – weak. Vibration type: ν – valence stretching.

cm⁻¹ (sugar-phosphate stretch), and 840 cm⁻¹ (phosphodiester mode) [55]. When a B to A transition occurs, B DNA marker bands at 840 cm⁻¹ and 1714 cm⁻¹ shift toward lower frequencies, and the 1222 cm⁻¹ band shifts to higher frequencies of about 1230–1240 cm⁻¹ [53,56]. In a B-to-Z transition, the band at 840 cm⁻¹ displaces to approximately 800 cm⁻¹, and the band at 1714 cm⁻¹ appears near 1690 cm⁻¹, whereas the band at 1222 cm⁻¹ shifts toward 1215 cm⁻¹ [57]. The changes observed in the bands at 1714 cm⁻¹ and 1222 cm⁻¹ do not indicate DNA conformational change. The slight spectral change recorded in the deoxyribose region 900–100 cm⁻¹ may be attributed to minor alterations in the sugar-phosphate geometry while DNA remains in B conformation [55].

3.5.4. FIP incorporation into the DNA

Fig. 6 (top) shows the spectral profiles of FT-IR spectra FIP in aqueous solution and FIP/DNA complex. The tentative assignment of the vibrational bands for the FIP molecule was made based on the data found in the literature [58]. Briefly, the FT-IR spectrum of FIP is dominated by a group of bands appearing in the region of 800–1100 cm⁻¹, which are attributed to S=O (1049 cm⁻¹) stretching vibrations (Table 2). The bands at 1143 cm⁻¹ and 1188 cm⁻¹ attend to the bending vibrations of functional groups C–F. These bands can be employed as an actual fingerprint region to carry out the FT-IR detection of FIP. The FT-IR spectrum of FIP also includes strong stretching bands at 883 cm⁻¹ and 1090 cm⁻¹ attributed to the vibrations in the heterocycle moiety of the molecule. FIP exhibits weak extra bands appearing at 1467 cm⁻¹ and 1582 cm⁻¹, corresponding to the C=C–N and C=C localized in the adjacent cycle of the molecule respectively. Finally, the bands observed between the two regions mentioned above correspond to C=C stretching vibration in heterocycle (1376 cm⁻¹) and bending vibration of the NH₂ group linked to the aromatic cyclic structure (1323 cm⁻¹) of the analyzed pesticide molecule (Table 2).

The interaction DNA macromolecule with FIP molecule indicates structural changes within FIP molecule manifested in its FT-IR spectrum. We observed the following significant changes by comparing the measured spectra for free FIP and FIP/DNA complex (Fig. 6, top). In the complex spectrum, relative enhancements of bands at 883, 1049, 1090, 1323, and 1376 cm⁻¹ can be seen, with a band shift of the 883 cm⁻¹ toward 877 cm⁻¹, 1049 cm⁻¹ to 1045 cm⁻¹, 1090 cm⁻¹ toward 1085 cm⁻¹, as well as bands at 1323 cm⁻¹ and 1376 cm⁻¹ shift to 1321 cm⁻¹ and 1383 cm⁻¹ respectively. We also recorded the loss of vibrational bands at 1143 cm⁻¹ and 1188 cm⁻¹ corresponding to functional groups C–F. The complete disappearance of the vibrations belonging to the C–F functional groups can be attributed to the interaction of FIP through the ends of its molecule where the fluorine atoms are located (Fig. 1). This claim is supported by the fact that fluorine is a highly electronegative element. The C=C vibration in the heterocycle (1376 cm⁻¹) relaxes, and the C=C bond wavenumber of the aromatic ring remains unchanged, which could indicate that the FIP molecule is rotated during

incorporation which leads to the fact that aromatic rings are oriented outward from the DNA groove (probably the minor groove, as shown by the above-mentioned results). From the point of view of DNA vibrations changes formed because of FIP incorporation, the cytosine (1489 cm⁻¹) and guanine (1714 cm⁻¹) vibrations shifted to lower values. This fact allows us to predict a binding of FIP on the G-C pairs levels. If we consider, the facts that the G-C regions in the B form of DNA are wider and FIP molecules are bigger than small planar aromatic molecules [59] then our above-mentioned claim seems to be conclusive. In conclusion, from the FT-IR analysis, it is possible to propose an interaction model for DNA + FIP as follows: the interaction is realized by hydrogen bonds between G-C pairs in the minor groove of the DNA macromolecule and the CF₃ functional groups of the aromatic heterocyclic ring of the FIP molecule.

3.6. Circular dichroism (CD) measurements

The circular dichroism method is very useful in studying the structural, morphological, and conformational changes of a DNA molecule caused by drug interaction or another small ligand [60]. This technique is excellent for rapidly evaluating the secondary structure and its changes [61]. CD spectra of the B form of DNA are characterized by a positive band at 275 nm due to base-stacking and a negative band at 245 nm resulting from right-handed helicity [62]. The simple groove binding and electrostatic interaction of small molecules has been proven to show less or no perturbation on the base-stacking and helicity bands [63]. The decrease of CD spectra at 275 nm and a slight change in the shape of the positive band were obtained upon the addition of small molecules like bisphenol A which indicates its binding to the DNA by intercalating. This reaction was realized between adjacent base pairs and induced a conformational change of DNA. In contrast, the enhancement of the intensity band at 275 nm and the shape change of the positive band predicts the binding of the small molecule, like acrylamide, into the minor groove of DNA [64].

The changes in the CD spectra of DNA in the presence of increasing concentrations of FIP are shown in Fig. 7. From our results, FIP causes only very slight, weak changes in the CD spectra of the DNA molecule. To better characterize the CD changes, we also calculated the molecular ellipticities of the two characteristic DNA bands (Table 3).

Molecular ellipticity values were calculated using the equation [65].

$$[\theta]_{\lambda} = \frac{100 \theta_{(\lambda)}}{cl} \quad (5)$$

where $[\theta]_{\lambda}$ represents the molecular ellipticity at a particular wavelength expressed in deg cm² dmol⁻¹, l is the length of the cell in cm, c corresponds to the concentration in moles of nucleotide phosphate per liter, and $\theta_{(\lambda)}$ is the observed rotation in degrees.

Based on the observed changes (Fig. 7, Table 3) and following the published knowledge mentioned above, we can conclude that the DNA

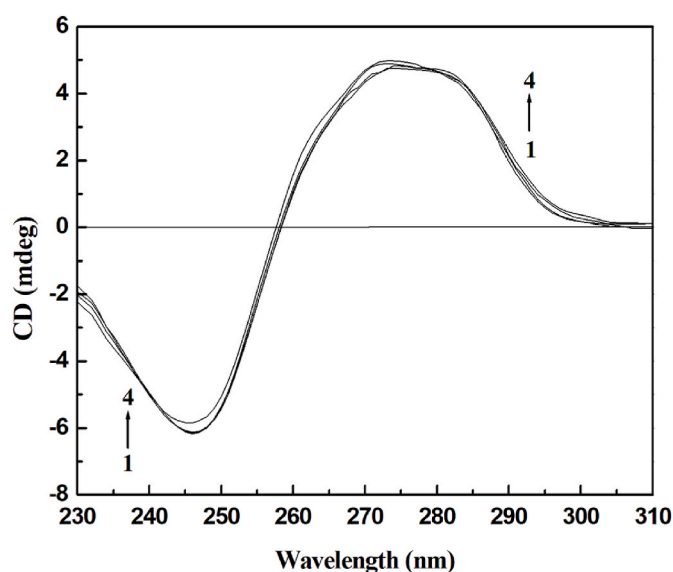


Fig. 7. CD spectra of DNA in the presence of increasing amounts of FIP at pH 7.4 and laboratory temperature. $c(\text{DNA}) = 2.4 \times 10^{-4}$ mol/L, $c(\text{FIP}) = 2.4 \times 10^{-4}$ – 7.2×10^{-4} mol/L; $[\text{DNA}]/[\text{FIP}] = 1/0, 1/1, 1/2, 1/3$.

Table 3

CD parameters for the interaction of DNA with FIP complexes.

Sample DNA/FIP	Molecular ellipticities $\theta_{275 \text{ nm}}$ (deg cm ² dmol ⁻¹)	Molecular ellipticities $\theta_{245 \text{ nm}}$ (deg cm ² dmol ⁻¹)
1/0	9906	-12186
1/1	10071	-12871
1/2	10188	-12817
1/3	10351	-12759

molecule does not significantly change its secondary structure in the presence of FIP, remaining in the B-form. The observed spectral changes are due to local disturbances in the geometry of the DNA bases rather than changes in the helical structure of the DNA [66]. Moreover, we observed a slight increase in the intensity of the band at 275 nm and a mild change in the shape of this positive DNA band, indicating that the local disturbances in the geometry of the DNA bases are probably caused by the FIP incorporation into the DNA molecule in its minor groove by forming hydrogen bonds between the CF₃ group of FIP and -NH group of DNA bases.

4. Comparison of fipronil – DNA interaction with other insecticides

The study of the interaction between insecticides and nucleic acid is considered to be important to allow screening for carcinogenic properties of pesticides in general [67,68]. Studies addressing the specific mode of interaction and binding sites of phenylpyrazoles insecticides with DNA are few. One group which has been studied is the group of neonicotinoid insecticides such as thiacloprid, imidacloprid, thiamethoxam and acetamiprid. The binding constant values of thiacloprid [47], thiamethoxam [69] and acetamiprid [70] when they interact with DNA are similar to that of fipronil and they are in order more than 10³ L/mol. The presence of both thiacloprid and fipronil causes a decrease in melting point temperature T_m and Van't Hoff enthalpy ΔH of DNA. These changes of thermodynamic parameters lead to destabilization of the DNA molecule. However, it was recorded a two-phase character melting curve of the complex DNA-thiacloprid with an expression destabilization of AT regions in DNA [47]. Although, both molecules are incorporated into DNA minor groove, thiacloprid prefers the regions rich in AT-base pairs, meanwhile fipronil that ones rich in GC-base pairs.

The situation with acetamiprid is different. This molecule stabilizes DNA as its melting point temperature increases after adding insecticide. The model in which it binds to DNA is a partial intercalation to the regions rich in GC-base pairs and its binding leads to a change in the secondary structure of DNA from B conformation to the A [70]. Jameel M. et al. [69] have investigated hazardous effect of thiametoxam on biochemical and biological parameters of the exposed insect organism from view of its interaction with DNA. When they measured a thiametoxam influence on DNA molecule they used calf thymus DNA in their spectroscopic experiments and postulated the same interaction mode as we got for fipronil.

Another group of pesticides is a group of conazole triazole fungicides including epoxiconazole and prothioconazole. Preliminary experiments obtained by spectroscopic and hydrodynamic methods show similar results as the investigation of the DNA-fipronil complex. The values of their binding constant does not point to an intercalation mode the interaction but the incorporation into the groove of DNA molecule (unpublished results).

From above mentioned studies we can suppose that heterocyclic ring in the structure of fipronil, thiacloprid, thiametoxam and triazole fungicides plays an important role in their mode of interaction with DNA. Only acetamipride is missing this ring and contains free linear sequention, which probably is a reason for its partial intercalation in the DNA structure.

5. Conclusions

Our work focused on monitoring changes in DNA structure and stability caused by phenylpyrazole insecticide FIP. The structure of the FIP molecule is a crescent shape due to the pulling of the sulphur atom inside the molecule. FIP is polar, well soluble in polar solvents and its magnitude of the dipole moment is 5.537 D. By increasing the DNA concentration, we detected a hyperchromic effect of the intensity absorbance of FIP, suggesting that FIP interacts with DNA differently than in intercalation mode. The strength of FIP binding to DNA is characterized by a binding constant comparable to the ligands binding to the DNA groove. The presence of DNA causes combined dynamic and static fluorescence quenching of FIP. At low concentrations, DNA is in contact with FIP without any change in the structure of the interacting molecules. At higher concentrations, DNA generates a non-fluorescent complex with FIP. The phenylpyrazole insecticide FIP destabilizes DNA structure, as shown by the observed decrease in all thermodynamic parameters. At the same time, we also observed a slight change in DNA viscosity in the presence of FIP. However, we can conclude that FIP does not cause significant conformational changes in DNA structure through its interaction, nor does it increase its chain length. The results allow us to assume that the phenylpyrazole insecticide FIP is incorporated into the groove of the DNA macromolecule via hydrogen interactions. FT-IR and CD measurements further specified the site of FIP incorporation into DNA and are consistent with the other results. The most likely site of FIP binding is a minor groove in the DNA macromolecule. FIP binds via hydrogen bonds between the CF₃ group of FIP and the nitrogenous bases of DNA.

In conclusion, we can state that through its interaction, FIP causes a change in the native DNA structure. As can be seen from other investigations, the fipronil mode of interaction with DNA is very similar to structuraly and functionaly like insecticide molecules such as some neonicotinoids or triazoles. Uncontrolled use of insecticides such as FIP can affect population dynamics at both the structural and functional levels. Proper use of insecticides, coupled with a well-studied mechanism of action, can significantly reduce their adverse effects on a population.

Funding

This work was funded by Operational Programme Integrated

Infrastructure, the projects ITMS: 313011AUW7 (NANOVIR) and ITMS: 313011AVG3 (BIOVID), co-funded by ERDF.

CRedit authorship contribution statement

Valéria Verebová: Writing – original draft, Visualization, Software, Resources, Formal analysis, Data curation. **Zdenka Bedlovičová:** Validation, Software, Investigation, Formal analysis, Data curation. **Zuzana Bednáriková:** Validation, Supervision, Project administration, Funding acquisition, Data curation. **Jana Stančíková:** Writing – review & editing, Supervision, Resources, Investigation, Conceptualization.

Data availability

Data will be made available on request.

Acknowledgements

The authors would like to thank their colleagues at the Centre for Interdisciplinary Biosciences for possibility to perform fluorescence measurements and the Department of Biophysics at the Slovak Academy of Sciences (Košice, Slovakia) for providing the opportunity to realize CD and FT-IR experiments and student Laura Tomkova for her help during the experiments.

References

- [1] C. Vidau, J.L. Brunet, L.P. Belzunces, Phenylpyrazole insecticides induce cytotoxicity by altering mechanisms involved in cellular energy supply in the human epithelial cell model Caco-2, *Toxicol. Vitro* 23 (2009) 589–597, <https://doi.org/10.1016/j.tiv.2009.01.017>.
- [2] G.W. Ware, D.M. Whitacre, *An Introduction to Insecticides, sixth ed.*, Meister Media Worldwide, Ohio, 2008, p. 496. US.
- [3] J.Z. Magalhães, T.M. Sandini, M.S.B. Udo, R.A. Fukushima, H. Spinoza, Fipronil: uses, pharmacological and toxicological features, *Revinter* 11 (2018) 67–83, <https://doi.org/10.22280/revintervol11ed1.344>.
- [4] D. Jiang, X. Zheng, G. Shao, Z. Ling, H. Xu, Discovery of a novel series of phenyl pyrazole inner salts based on fipronil as potential dual-target insecticides, *J. Agric. Food Chem.* 62 (2014) 3577–3583, <https://doi.org/10.1021/jf405512e>.
- [5] D. Gibbons, C. Morrissey, P. Mineau, A review of the direct and indirect effects of neonicotinoids and fipronil on vertebrate wildlife, *Environ. Sci. Pollut. Res.* 22 (2015) 103–118, <https://doi.org/10.1007/s11356-014-3180-5>.
- [6] D. Hainzl, L.M. Cole, J.E. Casida, Mechanisms for selective toxicity of fipronil insecticide and its sulfone metabolite and desulfinyl photoproduct, *Chem. Res. Toxicol.* 11 (1998) 1529–1535, <https://doi.org/10.1021/tx980157i>.
- [7] L. Chen, K.A. Durkin, J.E. Casida, Structural model for γ -aminobutyric acid receptor noncompetitive antagonist binding: widely diverse structures fit the same site, *Proc. Natl. Acad. Sci. U.S.A.* 103 (2006) 5185–5190, <https://doi.org/10.1073/pnas.0600370103>.
- [8] Y. Zhang, X. Meng, Y. Yang, H. Li, X. Wang, B. Yang, J. Zhang, C. Li, N.S. Millar, Z. Liu, Synergistic and compensatory effects of two point mutations conferring target-site resistance to fipronil in the insect GABA receptor RDL, *Sci. Rep.* 6 (2016) 32335, <https://doi.org/10.1038/srep32335>.
- [9] C.C.D. Tingle, J.A. Rother, C.F. Dewhurst, S. Lauer, W.J. King, Fipronil: environmental fate, ecotoxicology, and human health concerns, *Rev. Environ. Contam. Toxicol.* 176 (2003) 1–66, https://doi.org/10.1007/978-1-4899-7283-5_1.
- [10] C.C.D. Tingle, J.A. Rother, C.F. Dewhurst, S. Lauer, W.J. King, Health and environmental effects of fipronil, Briefing paper for Pesticides Action Network, UK 22 (2000) 103–118. <http://www.pan-uk.org/Publications/Briefing/fipronil.pdf>.
- [11] P.C. Badgujar, N.N. Pawar, G.A. Chandratre, A.G. Telang, A.K. Sharma, Fipronil induced oxidative stress in kidney and brain of mice: protective effect of vitamin E and vitamin C, *Pestic. Biochem. Physiol.* 118 (2015) 10–18, <https://doi.org/10.1016/j.pestbp.2014.10.013>.
- [12] X.Q. Wang, Y.G. Li, S. Zhong, H. Zhang, X.Y. Wang, P.P. Qi, H. Xu, Oxidative injury is involved in fipronil-induced G2/M phase arrest and apoptosis in *Spodoptera Frugiperda* (Sf9) cell line, *Pestic. Biochem. Physiol.* 105 (2013) 122–130, <https://doi.org/10.1016/j.pestbp.2012.12.008>.
- [13] A. Lopez-Antia, M.E. Ortiz-Santaliestra, P.R. Camarero, F. Mougeot, R. Mateo, Assessing the risk of fipronil-treated seed ingestion and associated adverse effects in the red-legged partridge, *Environ. Sci. Technol.* 49 (2015) 13649–13657, <https://doi.org/10.1021/acs.est.5b03822>.
- [14] A. Çelik, S.Y. Ekinçi, G. Güler, S. Yıldırım, In vitro genotoxicity of fipronil sister chromatid exchange, cytokinesis block micronucleus test, and comet assay, *DNA Cell Biol.* 33 (2014) 148–154, <https://doi.org/10.1089/dna.2013.2158>.
- [15] X. Wang, L. Xu, C. Hao, C. Xu, H. Kuang, Circular dichroism-active interactions between fipronil and neuronal cells, *Environ. Sci. Technol.* 5 (2018) 500–507, <https://doi.org/10.1021/acs.estlett.8b00321>.
- [16] P.R. De Oliveira, G.H. Bechara, S.E. Denardi, R.J. Oliveira, M.I.C. Mathias, Genotoxic and mutagenic effects of fipronil on mice, *Exp. Toxicol. Pathol.* 64 (2012) 569–573, <https://doi.org/10.1016/j.etp.2010.11.015>.
- [17] M. Singh, P. Kaur, R. Sandhir, R. Kiran, Protective effects of vitamin E against atrazine-induced genotoxicity in rats, *Mutat. Res.* 654 (2008) 45–149, <https://doi.org/10.1016/j.mrgentox.2008.05.010>.
- [18] P. Badgujar, N. Selkar, G.A. Chandratre, N.N. Pawar, V.D. Dighe, S.T. Bhagat, A. G. Telang, G.R. Vanage, Fipronil-induced genotoxicity and DNA damage in vivo: protective effect of vitamin E, *Hum. Exp. Toxicol.* 36 (2017) 508–519, <https://doi.org/10.1177/0960327116655388>.
- [19] M. Jameel, M.F. Alam, H. Younus, K. Jamal, H.R. Siddique, Hazardous sub-cellular effects of fipronil directly influence the organismal parameters of *Spodoptera litura*, *Ecotoxicol. Environ. Saf.* 172 (2019) 216–224, <https://doi.org/10.1016/j.ecoenv.2019.01.076>.
- [20] J.M. Bonmatin, C. Giorio, V. Girolami, D. Goulson, D.P. Kreutzweiser, C. Krupke, M. Leiss, E. Long, M. Marzaro, E.A.D. Mitchell, D.A. Noome, N. Simon-Delso, A. Tapparo, Environmental fate and exposure; neonicotinoids and fipronil, *Environ. Sci. Pollut. Res.* 22 (2015) 35–67, <https://doi.org/10.1007/s11356-014-3332-7>.
- [21] P.S. Dorraji, F. Jalali, Investigation of the interaction of sertraline with calf thymus DNA by spectroscopic methods, *J. Braz. Chem. Soc.* 24 (2013) 939–945, <https://doi.org/10.5935/0103-5053.20130123>.
- [22] HyperChem(TM) Professional 8.0, Hypercube, Inc., 1115 NW 4th Street, Gainesville, Florida 32601, USA..
- [23] M.J.S. Dewar, E.G. Zebisch, E.F. Healy, J.J.P. Stewart, Development and use of quantum mechanical molecular models. 76. AM1: a new general purpose quantum mechanical molecular model, *J. Am. Chem. Soc.* 107 (1985) 3902–3909, <https://doi.org/10.1021/ja00299a024>.
- [24] J. Gonzalez-Garcia, R. Vilar, *Supramolecular principles for small molecule binding to DNA structure*, in: J.L. Atwood, G.W. Gokel, L.J. Barbour (Eds.), *Comprehensive Supramolecular Chemistry II*, Elsevier, Amsterdam, Netherlands, 2017, pp. 39–70.
- [25] C.V. Kumar, R.S. Turner, E.H. Asuncion, Groove binding of a styrylcyanine dye to the DNA double helix: the salt effect, *J. Photochem. Photobiol., A: Chem* 74 (1993) 231–238, [https://doi.org/10.1016/1010-6030\(93\)80121-O](https://doi.org/10.1016/1010-6030(93)80121-O).
- [26] R.N. Jadeja, S. Parihar, K. Vyas, V.K. Gupta, Synthesis and crystal structure of a series of pyrazolone based Schiff base ligands and DNA binding studies of their copper complexes, *J. Mol. Struct.* 1013 (2012) 86–94, <https://doi.org/10.1016/j.molstruc.2012.01.006>.
- [27] E.C. Long, J.K. Barton, On demonstrating DNA intercalation, *Acc. Chem. Res.* 23 (1990) 271–273, <https://doi.org/10.1021/ar00177a001>.
- [28] R.S. Kumar, S. Arunachalam, DNA binding and antimicrobial studies of some polyethyleneimine-copper (II) complex samples containing 1,10-phenanthroline and l-threonine as co-ligands, *Polyhedron* 26 (2007) 3255–3262, <https://doi.org/10.1016/j.poly.2007.03.001>.
- [29] Z. Chen, G. Zhang, X. Chen, W. Gao, A resonance light-scattering off-on system for studies of the selective interaction between Adriamycin and DNA, *Anal. Bioanal. Chem.* 402 (2012) 2163–2171, <https://doi.org/10.1007/s00216-011-5672-1>.
- [30] M.B. Gholivand, S. Kashanian, H. Peyman, H. Roshanfekr, DNA-binding study of anthraquinone derivatives using chemometrics methods, *Eur. J. Med. Chem.* 46 (2011) 2630–2638, <https://doi.org/10.1016/j.ejmech.2011.03.034>.
- [31] P.S. Jourdan, C.A. McIntosh, R.L. Mansell, Naringin levels in citrus tissues: II. quantitative distribution of naringin in citrus paradise MacFad, *Plant Physiol.* 77 (1985) 903–908, <https://doi.org/10.1104/pp.77.4.903>.
- [32] T. Tsuruo, H. Iida, S. Tsukagoshi, Y. Sakurai, Overcoming of vincristine resistance in P388 leukemia in vivo and in vitro through enhanced cytotoxicity of vincristine and vinblastine by verapamil, *Cancer Res.* 41 (1981) 1967–1972.
- [33] G. Zhang, P. Fu, L. Wang, M. Hu, Molecular spectroscopic studies of farrerol interaction with calf thymus DNA, *J. Agric. Food Chem.* 59 (2011) 8944–8952, <https://doi.org/10.1021/jf2019006>.
- [34] H.R. Deepa, J. Thipperudrappa, H.M. Suresh Kumar, A study on fluorescence quenching of a laser dye by aromatic amines in alcohols, *Can. J. Phys.* 93 (2015) 469–474, <https://doi.org/10.1139/cjp-2014-0190>.
- [35] J.B. Le Pecq, C. Paoletti, A new fluorometric method for RNA and DNA determination, *Anal. Biochem.* 17 (1966) 100–107, [https://doi.org/10.1016/0003-2697\(66\)90012-1](https://doi.org/10.1016/0003-2697(66)90012-1).
- [36] W.G. Van Sark, P.L. Frederix, A.A. Bol, H.C. Gerritsen, A. Meijerink, Blueing, bleaching, and blinking of single CdSe/ZnS quantum dots, *ChemPhysChem* 3 (2002) 871–879, [https://doi.org/10.1002/1439-7641\(20021018\)3:10<871::AID-CPHC871>3.0.CO;2-T](https://doi.org/10.1002/1439-7641(20021018)3:10<871::AID-CPHC871>3.0.CO;2-T).
- [37] J.J. Peterson, T.D. Krauss, Fluorescence spectroscopy of single lead sulfide quantum dots, *Nano Lett.* 6 (2006) 510–514, <https://doi.org/10.1021/nl0525756>.
- [38] J.R. Lakowicz, *Introduction to fluorescence*, in: J.R. Lakowicz (Ed.), *Principles of Fluorescence Spectroscopy*, Springer, Boston, US, 1999, pp. 1–23.
- [39] E. Perianu, I. Rau, L.E. Vujan, DNA influence on norfloxacin fluorescence, *Spectrochim. Acta Mol. Biomol. Spectrosc.* 206 (2019) 8–15, <https://doi.org/10.1016/j.saa.2018.07.092>.
- [40] Y. Ma, G. Zhang, J. Pan, Spectroscopic studies of DNA interactions with food colorant indigo carmine with the use of ethidium bromide as a fluorescence probe, *J. Agric. Food Chem.* 60 (2012) 10867–10875, <https://doi.org/10.1021/jf303698k>.
- [41] C.N. Pace, Measuring and increasing protein stability, *Trends Biotechnol.* 8 (1990) 93–98, [https://doi.org/10.1016/0167-7799\(90\)90146-O](https://doi.org/10.1016/0167-7799(90)90146-O).
- [42] W.D. Wilson, F.A. Tanius, M. Fernandez-Saiz, C.T. Rigel, Evaluation of drug-nucleic acid interactions by thermal melting curves, in: K.R. Fox (Ed.), *Drug-DNA Interaction Protocols. Methods in Molecular Biology*, Humana Press, Totowa, New Jersey, US, 1997, pp. 219–240.

- [43] Y. Sun, H. Zhang, S. Bi, X. Zhou, L. Wang, Y. Yan, Studies on the arctiin and its interaction with DNA by spectral methods, *J. Lumin.* 131 (2011) 2299–2306, <https://doi.org/10.1016/j.jlumin.2011.04.036>.
- [44] S. Bi, H. Zhang, C. Qiao, Y. Sun, C. Liu, Studies of interaction of emodin and DNA in the presence of ethidium bromide by spectroscopic method, *Spectrochim. Acta Mol. Biomol. Spectrosc.* 69 (2008) 123–129, <https://doi.org/10.1016/j.saa.2007.03.017>.
- [45] H. Ihmels, D. Otto, Intercalation of organic dye molecules into double-stranded DNA-general principles and recent developments, in: F. Würthner (Ed.), *Supermolecular Dye Chemistry. Topics in Current Chemistry*, Springer, Berlin, Heidelberg, Deutschland, 2005, pp. 161–204.
- [46] R. Lavery, B. Pullman, Molecular electrostatic potential on the surface envelopes of macromolecules: B-DNA, *Int. J. Quant. Chem.* 20 (1981) 259–272, <https://doi.org/10.1002/qua.560200123>.
- [47] V. Verebová, K. Želonková, B. Holečková, J. Staničová, The effect of neonicotinoid insecticide thiacloprid on the structure and stability of DNA, *Physiol. Res.* 68 (2019) S459–S466, <https://doi.org/10.33549/physiolres.934385>.
- [48] R. Manikandan, N. Chitrapriya, Y.J. Jang, P. Viswanathamurthi, Evaluation of DNA-binding, radical scavenging and cytotoxic activity of five coordinated Cd(II) complexes containing 2-acetylpyridine-N4-substituted thiosemicarbazone, *RSC Adv.* 3 (2013) 11647–11657, <https://doi.org/10.1039/c3ra40814k>.
- [49] B.K. Sahoo, K.S. Ghosh, R. Bera, S. Dasgupta, Studies on the interaction of diacetylcurcumin with calf thymus DNA, *Chem. Phys.* 351 (2008) 163–169, <https://doi.org/10.1016/j.chemphys.2008.05.008>.
- [50] H.Y. Alniss, Thermodynamics of DNA minor groove binders: perspective, *J. Med. Chem.* 62 (2018) 385–402, <https://doi.org/10.1021/acs.jmedchem.8b00233>.
- [51] C.N. N'soukpoé-Kossi, A.A. Ouameur, T. Thomas, A. Shirahata, T.J. Thomas, H. A. Tajmir-Riahi, DNA interaction with antitumor poluamine analogues: a comparison with biogenic poluamines, *Biomacromolecules* 9 (2008) 2712–2718, <https://doi.org/10.1021/bm800412r>.
- [52] D.K. Jangir, G.J. Tyagi, R. Mehrotra, S. Kundu, Carboplatin interaction with calf-thymus DNA: a FTIR spectroscopic approach, *J. Mol. Struct.* 969 (2010) 126–129, <https://doi.org/10.1016/j.molstruc.2010.01.052>.
- [53] S. Nafisi, F.G. Kahangi, E. Azizi, N. Zebarjad, Interaction of zanamivir with DNA and RNA: models for drug-DNA and drug-RNA bindings, *J. Mol. Struct.* 830 (2007) 182–187, <https://doi.org/10.1016/j.molstruc.2006.09.032>.
- [54] S.T. Saito, G. Silva, C. Pungartnik, M. Brendel, Study of DNA-emodin interaction by FTIR and UV-vis spectroscopy, *J. Photochem. Photobiol. B Biol.* 111 (2012) 59–63, <https://doi.org/10.1016/j.jphotobiol.2012.03.012>.
- [55] R. Marty, C.N. N'soukpoé-Kossi, D. Charbonneau, C.M. Weinert, L. Kreplak, H.-A. Tajmir-Riahi, Structural analysis of DNA complexation with cationic lipids, *Nucleic Acids Res.* 37 (2009) 849–857, <https://doi.org/10.1093/nar/gkn1003>.
- [56] S. Nafisi, Z. Norouzi, A comparative study on the interaction of *cis*- and *trans*-platin with DNA and RNA, *DNA Cell Biol.* 28 (2009) 469–477, <https://doi.org/10.1089/dna.2009.0894>.
- [57] S. Alex, P. Dupuis, FT-IR and Raman investigation of cadmium binding by DNA, *Inorg. Chim. Acta.* 157 (1989) 271–281, [https://doi.org/10.1016/S0020-1693\(00\)80552-6](https://doi.org/10.1016/S0020-1693(00)80552-6).
- [58] M.A. Mohamed, J. Jaafar, A.F. Ismail, M.H.D. Othman, M.A. Rahman, Fourier transform infrared (FTIR) spectroscopy, in: N. Hilal, A.F. Ismail, T. Matsuura, D. Oatley-Radcliffe (Eds.), *Membrane Characterization*, Elsevier Inc., Swansea, UK, 2017, pp. 3–29.
- [59] B.S.P. Reddy, S.M. Sondhi, J.W. Lown, Synthetic DNA minor groove-binding drugs, *Pharmacol. Therapeut.* 84 (1999) 1–111, [https://doi.org/10.1016/S0163-7258\(99\)00021-2](https://doi.org/10.1016/S0163-7258(99)00021-2).
- [60] P. Lincoln, E. Tuite, B. Norden, Short-circuiting the molecular wire: cooperative binding of Δ -[Ru(phen)₂dppz]²⁺ and Δ -[Rh(phi)₂bipy]³⁺ to DNA, *J. Am. Chem. Soc.* 119 (1997) 1454–1455, <https://doi.org/10.1021/ja9631965>.
- [61] N.J. Greenfield, Using circular dichroism spectra to estimate protein secondary structure, *Nat. Protoc.* 1 (2006) 2876–2890, <https://doi.org/10.1038/nprot.2006.202>.
- [62] V.I. Ivanov, L.E. Minchenkova, A.K. Schyolkina, A.I. Poletayer, Different conformations of double-stranded nucleic acid in solution as revealed by circular dichroism, *Biopolymers* 12 (1973) 89–110, <https://doi.org/10.1002/bip.1973.360120109>.
- [63] B. Norden, F. Tjernerl, Structure of methylene blue-DNA complexes studied by linear and circular dichroism spectroscopy, *Biopolymers* 21 (1982) 1713–1734, <https://doi.org/10.1002/bip.360210904>.
- [64] Y.L. Zhang, X. Zhang, X.C. Fei, S.L. Wang, H.W. Gao, Binding of bisphenol A and acrylamide to BSA and DNA: insights into the comparative interactions of harmful chemicals with functional biomacromolecules, *J. Hazard Mater.* 182 (2010) 877–885, <https://doi.org/10.1016/j.jhazmat.2010.06.131>.
- [65] G.D. Fasman, *Circular Dichroism and Conformational Analysis of Biomolecules*, Plenum Press, New York, US, 1996, pp. 433–465, 1996.
- [66] C. Braun, G. Jas, S. Choosakoonkriang, G. Koe, J. Smith, C. Middaugh, The structure of DNA within cationic lipid/DNA complexes, *Biophys. J.* 84 (2003) 1114–1123.
- [67] F. Ahamdi, N. Jamali, R. Morarian, B. Astinchap, Binding studies of pyriproxyfen to DNA by multispectroscopic atomic force microscopy and molecular modeling methods, *DNA Cell Biol.* 31 (2012) 259–268, <https://doi.org/10.1089/dna.2011.1303>.
- [68] F. Ahmadi, B. Jafari, M. Rahimi-Nasrabadi, S. Ghasemi, K. Ghanbari, Proposed model for in vitro interaction between fenitrothion and DNA, by using competitive fluorescence, 31P NMR, 1H NMR, FT-IR, CD and molecular modeling, *Toxicol. Vitro* 27 (2013) 641–650, <https://doi.org/10.1016/j.tiv.2012.11.004>.
- [69] M. Jameel, K. Jamal, M.F. Alam, F. Ameen, H. Younus, H.R. Siddique, Interaction of thiamethoxam with DNA: hazardous effect on biochemical and biological parameters of the exposed organism, *Chemosphere* 254 (2020) 126875, <https://doi.org/10.1016/j.chemosphere.2020.126875>.
- [70] Y. Zhang, G. Zhang, X. Zhou, Y. Li, Determination of acetamiprid partial-intercalative binding to DNA by use of spectroscopic, chemometrics, and molecular docking techniques, *Anal. Bioanal. Chem.* 405 (2013) 8871–8883, <https://doi.org/10.1007/s00216-013-7294-2>.